

Article

# Methodology for Evaluating the CO<sub>2</sub> Sequestration Capacity of Waste Ashes

Sara Tominc  and Vilma Ducman \* 

Laboratory for Cements, Mortars and Ceramics, The Department of Materials, Slovenian National Building and Civil Engineering Institute (ZAG), Dimičeva ulica 12, 1000 Ljubljana, Slovenia; sara.tominc@zag.si

\* Correspondence: vilma.ducman@zag.si; Tel.: +386-1-2804-438

**Abstract:** The concentration of CO<sub>2</sub> in the atmosphere is constantly increasing, leading to an increase in the average global temperature and, thus, affecting climate change. Hence, various initiatives have been proposed to mitigate this process, among which CO<sub>2</sub> sequestration is a technically simple and efficient approach. The spontaneous carbonation of ashes with atmospheric CO<sub>2</sub> is very slow, and this is why accelerated carbonation is encouraged. However, not all ashes are equally suitable for this process, so a methodology to evaluate their potential should be developed. Such a methodology involves a combination of techniques, from theoretical calculations to XRF, XRD, DTA-TG, and the calcimetric determination of the CaCO<sub>3</sub> content. The present study followed the approach of exposing ashes to accelerated carbonation conditions (4% v/v CO<sub>2</sub>, 50–55% and 80–85% RH, 20 °C) in a closed carbonation chamber for different periods of time until the maximum CO<sub>2</sub> uptake is reached. The amount of sequestered CO<sub>2</sub> was quantified by thermogravimetry. The results show that the highest CO<sub>2</sub> sequestration capacity (33.8%) and carbonation efficiency (67.9%) were obtained for wood biomass bottom ash. This method was applied to eight combustion ashes and could serve to evaluate other ashes or comparable carbon storage materials.

**Keywords:** CO<sub>2</sub> sequestration; carbonation efficiency; coal ash; wood biomass ash; co-combustion ash; DTA-TG analysis



**Citation:** Tominc, S.; Ducman, V. Methodology for Evaluating the CO<sub>2</sub> Sequestration Capacity of Waste Ashes. *Materials* **2023**, *16*, 5284. <https://doi.org/10.3390/ma16155284>

Academic Editor: Sylvia Boycheva

Received: 1 June 2023

Revised: 21 July 2023

Accepted: 25 July 2023

Published: 27 July 2023



**Copyright:** © 2023 by the authors. Licensee MDPI, Basel, Switzerland. This article is an open access article distributed under the terms and conditions of the Creative Commons Attribution (CC BY) license (<https://creativecommons.org/licenses/by/4.0/>).

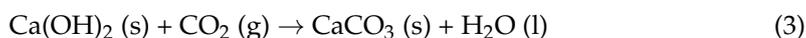
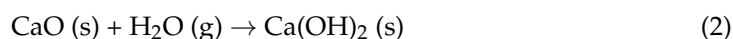
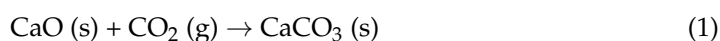
## 1. Introduction

The concentration of CO<sub>2</sub> in the atmosphere varies with global temperature but has not exceeded 300 parts per million (ppm) for thousands of years [1]. CO<sub>2</sub> emissions from fossil fuel industries can be a significant cause of CO<sub>2</sub> accumulation in the atmosphere, with more than 36 Gt CO<sub>2</sub>/year released globally from fossil fuel combustion, cement production, and other industrial processes [2]. For example, the CO<sub>2</sub> concentration was 280 ppm at the beginning of the Industrial Revolution but has steadily increased since then, while the use of conventional fossil fuels (i.e., coal, oil, and natural gas) became the main source of energy [3]. In 2016, the atmospheric CO<sub>2</sub> concentration exceeded 400 ppm [1,4]. Stern et al. [5] predicted that the CO<sub>2</sub> concentration could rise to over 550 ppm by 2050, and this would mean drastic global warming. CO<sub>2</sub> emissions have been increasing by about 1% per year, with only temporary decreases in 2020 and 2021 due to the COVID-19 pandemic [6–8]. In 2022, the atmospheric CO<sub>2</sub> concentration returned to 420 ppm, and in 2023, CO<sub>2</sub> emissions reached a record level [9,10].

Several initiatives have been proposed to address the rising CO<sub>2</sub> concentrations. A strategy based on CO<sub>2</sub> capture and utilization (CCU) is considered a promising way to reduce CO<sub>2</sub> emissions and is in line with the basic principle of industrial ecology, which nearly closes material cycles [11,12]. Besides CCU, carbon capture and storage (CCS) is also considered to be a promising strategy to reduce CO<sub>2</sub> emissions [11]. One of the CCS methods is storing CO<sub>2</sub> in former oil or gas reservoirs with impermeable cap rock under high pressure [13]. Biomass has additional CCS potential due to the sequestration of

atmospheric CO<sub>2</sub> in biomass ash, and a sustainable industrial production of bioenergy can reduce CO<sub>2</sub> emissions and minimize the use of expensive CCS technologies [14]. The combination of both approaches is called carbon capture, utilization, and storage (CCUS) and includes pipelines for transportation; injecting CO<sub>2</sub> into geological formations for storage; and finally its utilization for fuel, chemical, or material products with the potential to reduce about 19% of the global CO<sub>2</sub> output by 2050 [9]. The cost of CO<sub>2</sub> capture reached around USD 60–110/t globally in 2022 and is projected to halve by 2030. Reducing costs would allow an increased implementation of these technologies on an industrial scale [9].

In contrast to existing energy- and cost-intensive carbon capture and storage technologies, CO<sub>2</sub> mineral sequestration represents a low-tech approach that mainly involves the reaction of CO<sub>2</sub> with Ca- and Mg-rich minerals and the formation of carbonate minerals, e.g., calcite (CaCO<sub>3</sub>), magnesite (MgCO<sub>3</sub>), and dolomite (CaMg(CO<sub>3</sub>)<sub>2</sub>) [2,13,15]. Spontaneous carbonation with atmospheric CO<sub>2</sub> (0.04%) is generally very slow, so the natural CO<sub>2</sub> sequestration is insufficient [15–17]. Carbonation can be accelerated by an increased concentration or pressure of CO<sub>2</sub>. Combustion residues react with CO<sub>2</sub>, where the most common component is the strongly basic calcium oxide (CaO; Equation (1)) [18]. Directly binding molecular CO<sub>2</sub> to CaO is a very slow process, and the reaction is faster in the presence of H<sub>2</sub>O (liquid water or moisture) [15]. Here, CO<sub>2</sub> first dissolves in H<sub>2</sub>O, dissociates, and reacts with Ca-hydroxide to form CaCO<sub>3</sub>, which has very low solubility in H<sub>2</sub>O (Equations (2) and (3)) [18]. This process changes the chemical and physical properties of the ash.



CO<sub>2</sub> mineral sequestration is a method that involves the conversion of CO<sub>2</sub> into stable mineral carbonates and their subsequent storage. The reaction of CO<sub>2</sub> with minerals can occur without external energy input [19]. Direct mineral carbonation treatment can be divided into dry (or gas–solid) carbonation under a certain relative humidity and aqueous (or fluid–solid) carbonation, in which mineral wastes are immersed in a liquid mixture injected with gaseous CO<sub>2</sub> [19]. Direct aqueous carbonation is an efficient method for sequestration, and improved reaction kinetics can be achieved by using additives or maximizing temperature and pressure values. However, the increase in the reaction temperature and the complicated operating process limits its use [20]. It is also expensive compared to dry carbonation [19]. The main advantages of carbonation are the high stability of the main product (CaCO<sub>3</sub>), meaning that CO<sub>2</sub> is unlikely to be released under normal conditions. The reaction is exothermic and requires no additional energy input. The high availability of ashes as by-products of solid fuel combustion is also an advantage [13,21].

The carbonation process also enables us to lower the values of critical parameters such as alkalinity and solubility, which limit the disposal of wood ash in landfills. As spontaneous carbonation is quite slow and ineffective due to the low relative CO<sub>2</sub> content in air [22], it can be improved by accelerated carbonation, i.e., direct exposure to CO<sub>2</sub> in the closed chamber, resulting in a higher carbonation rate. The rate of the accelerated carbonation reaction can be determined by the reactivity of CO<sub>2</sub>, which is influenced by the carbonation conditions, such as the particle size of the material (i.e., reaction interface), relative humidity (RH), temperature, contact time, pressure, and CO<sub>2</sub> concentration [22–24]. The applicability of accelerated carbonation depends on the choice of appropriate exposure conditions [16]. In this context, the RH condition is essential to the reaction kinetics. Studies have shown that the reaction rate and the conversion rate of Ca(OH)<sub>2</sub> increase with increasing RH (up to 91%) [25,26]. Thus, complete carbonation can be achieved at a high RH.

Carbonation is one of the most discussed research topics in the cement and concrete industry. Almost all cement-based materials must undergo a carbonation reaction during their lifetime due to the CO<sub>2</sub> content in earth's atmosphere [16]. When CO<sub>2</sub> diffuses into the concrete, carbonation occurs, and the pH of the concrete decreases to about 9–10. At such a relatively low pH, the existing passive protective layer on the steel surface breaks down and corrosion occurs [17]. Thus, the carbonation reaction of concrete reduces the durability of such materials, while the carbonation reaction in alkali-activated materials (AAMs) poses an even greater risk; it disintegrates the binder matrix and, thus, reduces its strength [16]. However, studies show that using 10% carbonated fly ash as a partial cement replacement is comparable to the early compressive-strength results of mortars without fly ash [15,27]. After accelerated carbonation curing, a 15 kg concrete block (with 13% cement) can store up to 0.47 kg of CO<sub>2</sub>, assuming 24% CO<sub>2</sub> uptake by the cement [16,28]. Accordingly, carbon emissions from the cement industry could be reduced by 2.5% at the same carbon uptake rate if the cement industry used carbonation curing [28].

Using CO<sub>2</sub> sequestration for the production of building materials may be the only economically sustainable carbon-negative industrial process and, therefore, deserves to be the focus of further development [18]. A promising option is the replacement of cement in specific applications with alternative binders, using carbstone technology, a new method that is much more environmentally friendly, as no cement or concrete products are used [29,30]. Ghent is the first Belgian city to build a circular footpath with clinkers produced using the carbstone technology. Bricks are produced by reacting residues from the steel industry (steel slag) with CO<sub>2</sub>. The carbstone technology is based on the reaction of Ca- and Mg-containing minerals with CO<sub>2</sub> to form carbonate binders [30]. Other potential sources from waste streams are ashes containing Ca and Mg compounds, which allow for the sequestration of CO<sub>2</sub> in the form of carbonate compounds [15,31]. Therefore, wood biomass ash (WBA) is an attractive candidate for CO<sub>2</sub> sequestration as a Ca-rich ash [13,32]. In total, 70% of WBA is still landfilled, although it is a potential substitute material in various construction sectors or for CO<sub>2</sub> sequestration [11,13,15,33].

Although CO<sub>2</sub> sequestration is a promising carbon capture and storage technology, not much is known about the sequestration potential of various waste ashes. Tamiselvi Dananjayan et al. [34] reported the highest carbonation efficiency (CE) of coal fly ash (67.87%) achieved by the aqueous carbonation route under optimized process conditions (4 bar pressure with 100% CO<sub>2</sub>). Liu et al. [20] reported a sequestration efficiency of 28.74% of fly ash in the circulating fluidized bed process with the addition of 20% H<sub>2</sub>O (g) by direct gas–solid carbonation, while Koch et al. [13] determined a low average CE of 16.44% for bottom wood ash at different mixing ratios with water in batch experiments.

The main objective of the work presented here is to provide a methodology for evaluating the sequestration capacity of (Ca-rich) combustion waste ashes by a one-step direct gas–solid carbonation process with controlled CO<sub>2</sub> concentration, temperature, and RH. Using a number of complementary analytical methods, including the mass gain method; calcimetric measurements; and DTA-TG, XRF, and XRD analyses, the degree of carbonation can be confirmed, and the maximum carbonation efficiency can be calculated, allowing the sequestration potential of each ash to be determined.

## 2. Materials and Methods

### 2.1. Materials

Eight ashes were studied (Figure 1), including two coal fly ashes from German (A1) and Slovenian thermal power plants (A2). Two other ashes (A3 and A4) originated from a Slovenian heat power station, with A3 representing fly ash and A4 bottom ash produced from the combustion of wood biomass (wood chips). Two more ashes came from a paper mill, where the fuel source for A5 fly ash is coal, biomass, and paper sludge, while the fuel source for A6 was fiber paper sludge, waste wood, and bark, resulting in a mixture of 90% bottom ash and 10% fly ash. The last two ashes were from a Slovenian combined heat and

power station, where the fuel source is brown coal and wood biomass–wood chips (15%); A7 is fly ash, while A8 is bottom ash.



**Figure 1.** Waste ashes from different sources: (a,b) fly ash from coal (A1 and A2), (c) fly ash (A3) and (d) bottom ash from wood (A4), (e) fly ash (A5) and (f) mixed ash (A6) from a paper mill, and (g) fly ash (A7) and (h) bottom ash (A8) from a Slovenian heating and power station.

## 2.2. Characterization

All ashes were homogenized by quartering, packed in a PVC bag, and stored in a plastic container.

The ashes were sieved below 63  $\mu\text{m}$  and placed in 27 mm holders for mineralogical analyses, which were performed before and after  $\text{CO}_2$  exposure by X-ray diffraction (XRD; Empyrean X-ray Diffractometer, Cu X-ray source; PANalytical, Almelo, The Netherlands) in  $0.013^\circ$  steps from angles of  $4\text{--}70^\circ$ , under clean room conditions, using the external standard method (corundum NIST SRM 676a). Mineral analyses were performed using the PANalytical X'Pert High Score Plus diffraction software v. 4.8.

The ashes were sieved below 125  $\mu\text{m}$  for chemical analyses, dried at  $105^\circ\text{C}$ , and heated at  $950^\circ\text{C}$  to determine their loss on ignition (LOI); a fused bead was then prepared with a mixture of ash and flux (50% lithium tetraborate/50% lithium metaborate) in a 1:10 ratio (0.947 g: 9.47 g) and heated at  $1100^\circ\text{C}$ . The standard deviation of repeatability for LOI is 0.04 mass percent according to the standard EN 196-2:2013 [35]. The chemical composition of the ashes was determined using a ARL PERFORM'X Wavelength Dispersive X-Ray Fluorescence Spectrometer (WDXRF; Thermo Fisher Scientific Inc., Ecublens, Switzerland) with an Rh-target X-ray tube and the UniQuant 5 software (Thermo Fisher Scientific Inc., Waltham, MA, USA). The free CaO content was determined according to the standard EN 451-1:2017 [36]. Two measurements were performed for each ash. A mixture of butanoic acid, 3-oxo-ethyl ester, and butan-2-ol was added to the weighed, homogenized sample, sieved under 63  $\mu\text{m}$ . The flask was fitted with the spiral reflux condenser and the absorption tube and boiled for 3 h. The warm mixture was filtered through a filter crucible, and the residue was washed with propan-2-ol. A few drops of bromophenol blue indicator were added to the filtrate, and the filtrate was titrated with HCl until the color changed to yellow. The free CaO content was expressed as a mass percent of dry ash. The standard deviation of repeatability for the determination of free CaO content is 0.03 mass percent.

The  $\text{CO}_2$  sequestration capacity of all ashes was first tested at a controlled RH of 50–55% and a temperature of  $20 \pm 1^\circ\text{C}$  and then at an elevated RH of 80–85%. The received ashes were sieved to a grain size below 125  $\mu\text{m}$  and exposed to  $4 \pm 0.1$  vol%  $\text{CO}_2$  for 28 days in a closed carbonation chamber. Samples were taken after 1, 7, 14, 21, and 28 days. The carbonated samples were dried at  $105^\circ\text{C}$  for 24 h for further analyses.

The dried and sieved carbonated ashes were analyzed using a pressure calcimeter (OFITE Calcimeter, OFI Testing Equipment Inc., Houston, TX, USA, according to ASTM D 4373) with an analytical error of <5%. In the OFITE Calcimeter, CaCO<sub>3</sub> reacted with 10% HCl in a closed reaction cell to form CaCl<sub>2</sub>, CO<sub>2</sub>, and H<sub>2</sub>O. The pressure of the released CO<sub>2</sub> was measured with a manometer. The calcimeter was calibrated by reacting HCl with pure CaCO<sub>3</sub> before the actual measurements.

A differential thermal and thermogravimetric analysis (DTA-TG) was performed on carbonated ashes, using a STA 409 PC Luxx Simultaneous thermal analyzer (Netzsch-Gerätebau GmbH, Selb/Bayern, Germany) from 25 to 1000 °C, with a heating rate of 10 K min<sup>-1</sup>. Prior to the measurements, the ashes were dried at 105 °C and sieved below 63 μm. To prevent oxidation during the measurement, the sample chamber was filled with N<sub>2</sub> with a flow rate of 20 mL min<sup>-1</sup>. Ash batches with an initial mass of 50 mg were placed in Al<sub>2</sub>O<sub>3</sub> crucibles. TG measured the weight loss in the temperature range of decomposition of the carbonate mineral (550–950 °C), with an analytical error of <1%. The results were analyzed using the Proteus Thermal Analysis software v. 5.2.0 (Netzsch-Gerätebau GmbH, Selb/Bayern, Germany) Each ash was analyzed separately.

The specific surface area was determined by using the Brunauer–Emmett–Teller (BET) method according to ISO 9277.2010, with a Micromeritics ASAP-2020 analyzer (Micromeritics, Norcross, GA, USA) The ash particle shape and size were determined by scanning electron microscopy (a JEOL IT500 LV SEM, Tokyo, Japan) The uncoated ash was placed on the holder and examined in low vacuum mode, using an accelerating voltage of 20 kV and a working distance of 10 mm.

### 2.3. CO<sub>2</sub> Sequestration Capacity and Carbonation Efficiency

The theoretical maximum of sequestered CO<sub>2</sub> was determined based on the chemical composition of the ashes in weight percent (wt%), using the Steinour stoichiometric formula (Equation (4)), as reported in the literature [13,16,23,37]:

$$\text{CO}_{2\text{-max}} (\text{wt}\%) = 0.785 (\text{CaO} - 0.7 \text{SO}_3) + 1.091 \text{MgO} + 0.935 \text{K}_2\text{O} + 1.420 \text{Na}_2\text{O} \quad (4)$$

The mass uptake (mass<sub>-uptake</sub>) was determined using the mass gain method, where m<sub>ash</sub> is the original mass of the waste ash before the carbonation treatment, and m<sub>CO<sub>2</sub></sub> is the mass of the CO<sub>2</sub> sequestered during the carbonation treatment (Equation (5)) [15]. The CO<sub>2</sub> sequestration capacity was determined using TG analysis. The carbonation efficiency (CE) was determined as the ratio between the percentage of CO<sub>2</sub> sequestered experimentally according to the TG analysis and the theoretical CO<sub>2</sub> value calculated using Steinour's equation (Equation (6)) [13]. Higher carbonation efficiency indicates better CO<sub>2</sub> sequestration [13].

$$\text{mass}_{\text{-uptake}} (\%) = m_{\text{CO}_2} / m_{\text{ash}} \times 100 \quad (5)$$

$$\text{CE} (\%) = \text{CO}_{2\text{-TG exp}} (\%) / \text{CO}_{2\text{-max}} (\%) \quad (6)$$

## 3. Results and Discussion

### 3.1. Chemical and Mineralogical Composition of the Analyzed Ashes

The XRF analysis of the ashes A1 and A2 showed that the coal ashes mainly consist of SiO<sub>2</sub>, Al<sub>2</sub>O<sub>3</sub>, Fe<sub>2</sub>O<sub>3</sub>, and CaO, while the other ashes had a significantly higher wt% content of CaO (especially A4, A5, and A6) and lower contents of Al<sub>2</sub>O<sub>3</sub>, Fe<sub>2</sub>O<sub>3</sub> (except A7), and SiO<sub>2</sub>. The WBAs (A3 and A4) mainly consist of CaO, Al<sub>2</sub>O<sub>3</sub>, K<sub>2</sub>O, MgO, and SiO<sub>2</sub>, as shown in Figure 2. The ashes A3-8 have high alkali metal contents, such as Ca and Mg, which are favorable for CO<sub>2</sub> sequestration. The mean values of the primary oxides measured by XRF and the LOI at 550 and 950 °C are given in Table 1.

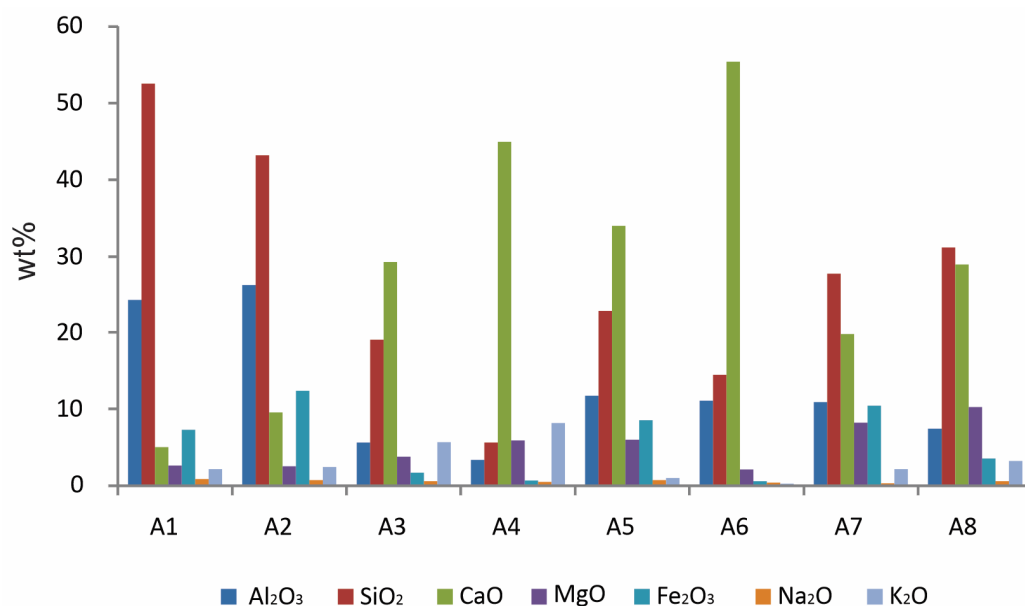


Figure 2. Comparison of the primary oxides of the studied ashes by XRF analysis.

Table 1. Specific surface area (BET), content of free CaO, loss on ignition (LOI) at 550 and 950 °C, and chemical composition of the original ashes in terms of the primary oxides (wt%), measured using XRF.

Ash Type:	Sample ID	Free CaO (%)	BET (m <sup>2</sup> /g)	LOI <sub>550 °C</sub>	LOI <sub>950 °C</sub>	Δ LOI(950–550 °C)	Al <sub>2</sub> O <sub>3</sub>	SiO <sub>2</sub>	CaO	MgO	Fe <sub>2</sub> O <sub>3</sub>	Na <sub>2</sub> O	K <sub>2</sub> O	P <sub>2</sub> O <sub>5</sub>	TiO <sub>2</sub>	SO <sub>3</sub>
Coal ash	A1	0.29	1.34	1.81	2.39	0.55	24.35	52.53	5.03	2.60	7.30	0.86	2.15	0.69	0.88	0.43
	A2	0.42	2.56	0.64	0.64	0.00	26.29	43.20	9.56	2.54	12.37	0.74	2.44	0.34	0.73	0.61
Wood ash	A3	4.61	3.80	13.91	29.91	16.00	5.62	19.04	29.27	3.78	1.70	0.56	5.65	2.24	0.37	1.00
	A4	16.74	41.83	2.26	26.09	23.83	3.35	5.64	44.95	5.88	0.68	0.48	8.14	2.82	0.07	0.32
Co-combustion ash	A5	8.06	41.29	5.20	11.71	6.51	11.71	22.90	34.01	5.99	8.53	0.74	0.99	0.28	0.73	1.70
	A6	20.63	6.36	0.00	14.55	14.55	11.08	14.45	55.40	2.12	0.56	0.41	0.25	0.26	0.22	0.20
	A7	5.11	86.07	11.68	16.98	5.30	10.87	27.78	19.77	8.21	10.44	0.28	2.16	0.56	0.52	1.69
	A8	13.24	5.75	0.38	12.79	12.41	7.43	31.17	28.98	10.25	3.56	0.57	3.21	1.00	0.32	0.07

Analyzing the crystal phases before the CO<sub>2</sub> exposure showed that the coal ashes mainly contain quartz, mullite, magnesioferrite, hematite, and anorthite, whereas WBA

mainly contains calcite, lime, portlandite, fairchildite, and quartz. The co-combustion ashes contain calcite, lime, quartz, anhydrite, periclase, and minor phases of portlandite, hematite, brownmillerite, akermanite, and larnite. According to the literature, possible carbonation minerals are Ca and Mg oxides (lime and periclase), hydroxides (portlandite), sulfates (anhydrite), and silicates [38,39].

The physical and chemical properties of ash are significantly affected by the type of combustion technology from which it originates [40]. In our study, fly ash from wood biomass (A3) had a much lower specific surface area than bottom ash from wood biomass (A4; Table 1), which was also confirmed by SEM (Figure 3). Larger particles are generally considered to be less reactive to CO<sub>2</sub> and have a lower specific surface area [22,41]. In our case, the ashes A4, A5, and A7 had a much larger specific surface area than the others, which could affect their reactivity to CO<sub>2</sub>.

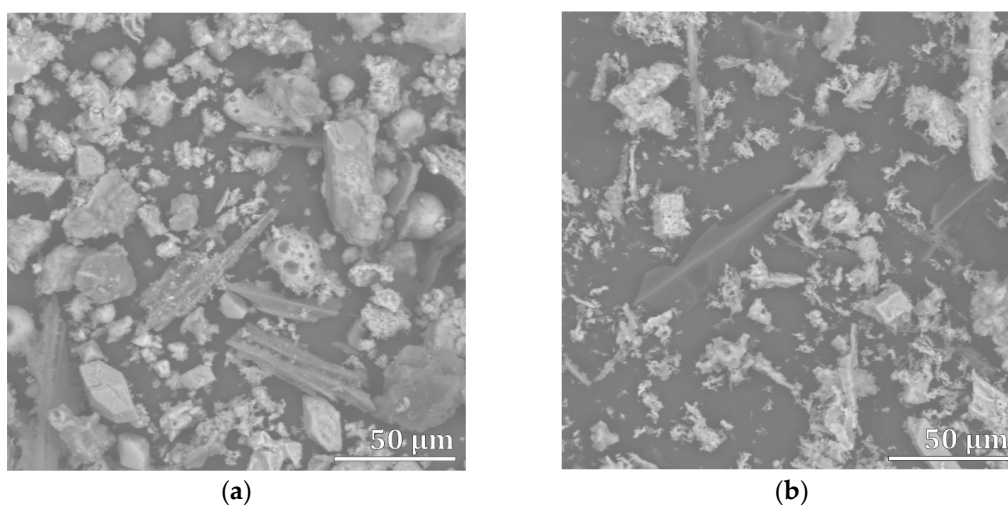


**Figure 3.** SEM micrographs of (a) wood biomass fly ash (A3) and (b) wood biomass bottom ash (A4).

The approach adopted in this study is the so-called “reverse” analysis. All received ashes, even directly from the production line, but especially if stored for some time, already experienced a certain degree of carbonation. Therefore, it would be incorrect to base the calculations on the carbonate content at the beginning of the measurements and after the exposure. Instead, the complete carbonation must be addressed, and then the maximum potential for CO<sub>2</sub> sequestration must be evaluated.

According to the analysis of the crystalline phases, the most obvious differences between the X-ray diffractograms of the ashes after 28 days of CO<sub>2</sub> exposure were in the presence of calcite and lime peaks (Figure 4). After 28 days of CO<sub>2</sub> exposure and an RH of 80–85%, the intensity of the lime peaks decreased significantly. A similar drop in intensity is observed for ash A6. In both samples (A4 and A6), calcite is already present before CO<sub>2</sub> exposure, meaning that the ash is already partially carbonated. However, with exposure to CO<sub>2</sub> and an increase in RH (80–85%), the intensity of the calcite peaks increases significantly. Thus, the XRD analysis allows us to follow the carbonation process and the relative content of the calcite/lime.

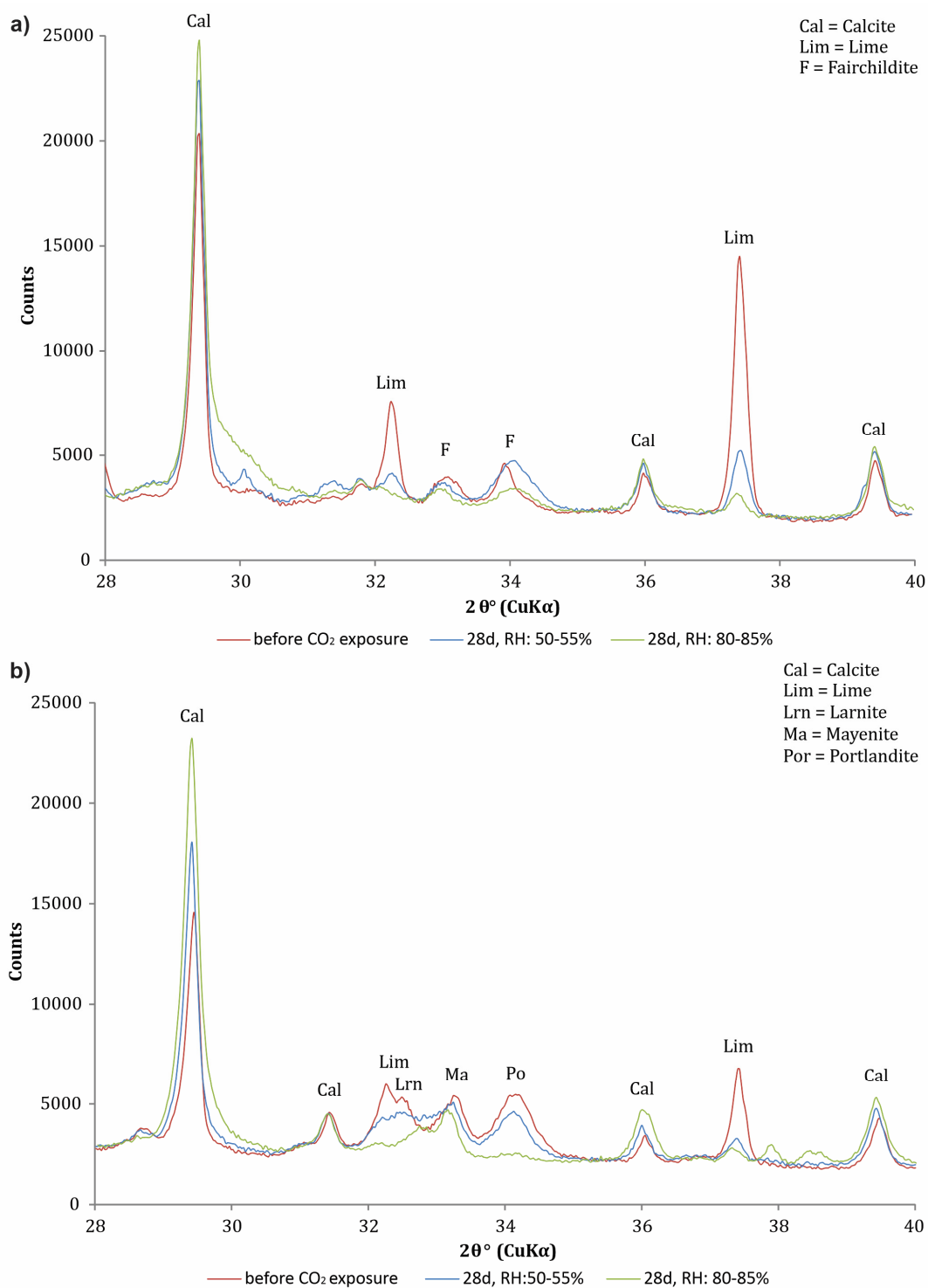


**Figure 4.** X-ray diffractograms of (a) A4 and (b) A6 before and after 28 days of CO<sub>2</sub> exposure at an RH of 50–55% and 80–85%, respectively. The main peaks of calcite (Cal) are marked at  $2\theta \approx 29.4^\circ$ ,  $36.0^\circ$ , and  $39.4^\circ$ ; and for lime (Lim), they are marked at  $2\theta \approx 32.2^\circ$  and  $37.4^\circ$ .

We also observed other possible carbonation minerals, such as portlandite (Ca(OH)<sub>2</sub>). Many authors have studied the carbonation of portlandite at different RHs and found that the carbonation of portlandite can be avoided at a low RH, while at a very high RH (>90%), the water film on the surface of portlandite consists of a larger number of water monolayers, allowing CaCO<sub>3</sub> to nucleate in the aqueous layer and at the crystal/solution

interface [25,26,42,43]. In addition to a faster reaction, complete carbonation can be achieved at a high RH [26], and we were able to confirm this with our X-ray diffractograms. After 28 days of CO<sub>2</sub> exposure, portlandite is no longer detectable at an RH of 80–85%, while at an RH of 50–55%, the peak is still very prominent (Figure 4b).

### 3.2. Calcimetric Measurements

The trend of increasing CaCO<sub>3</sub> content was monitored by calcimetric measurements. Figure 5 shows that the CaCO<sub>3</sub> content increased rapidly during the first week of CO<sub>2</sub> exposure and then increased very slowly. When the CaCO<sub>3</sub> content stops increasing, maximum carbonation is reached. After 28 days of CO<sub>2</sub> exposure at an RH of 50–55%, the curve for ashes A4 and A6 still increased slightly, indicating that maximum carbonation was not yet reached for these ashes. The calcimetric measurements are consistent with the X-ray diffractograms in Figure 4, where the lime and portlandite peaks are still clearly visible after 28 days of CO<sub>2</sub> exposure at an RH of 50–55%. However, when the RH was increased to 80–85%, the CaCO<sub>3</sub> content stopped increasing (Figure 5b), indicating that maximum carbonation was achieved.

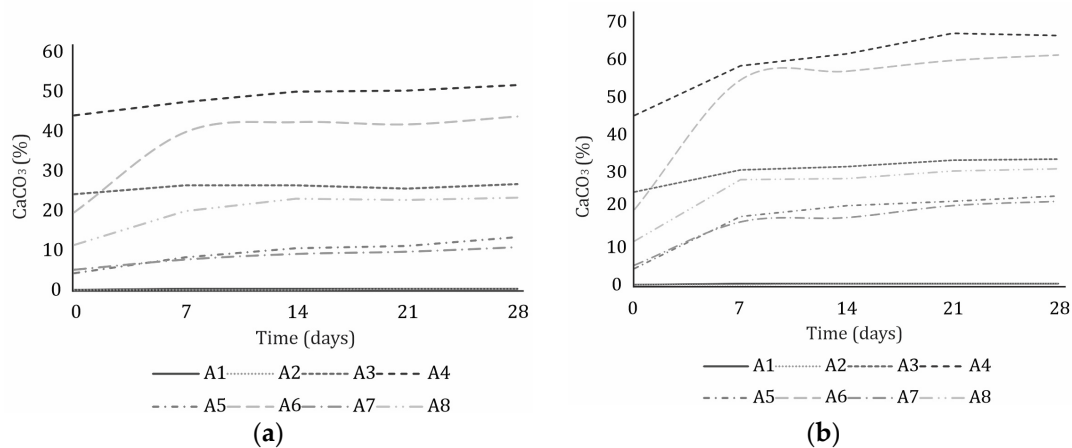
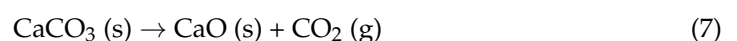


**Figure 5.** CaCO<sub>3</sub> content in ashes A1–8 during 28 days of CO<sub>2</sub> exposure in the carbonation chamber (a) at an RH of 50–55% and (b) 80–85%.

### 3.3. DTA-TG Analysis

Thermogravimetry (TG) measures the mass change of a sample when it is subjected to a temperature program in a controlled atmosphere [44]. Because of possible hydration reactions contributing to the weight gain, TG is a suitable method to quantify the increase in the CaCO<sub>3</sub> content during carbonation and provides quantitative information on the extent of carbonation [16,22]. Figure 6 shows the (a) TG and (b) DTA analysis for carbonated ashes after 28 days of CO<sub>2</sub> exposure at RH of 50–55%, and Figure 7 at RH of 80–85%. The weight loss measurements in the temperature range of 550–950 °C provide information about the amount of sequestered CO<sub>2</sub>.

Three main peaks can be observed on the DTA diagram. The first peak, which is below 200 °C, can be attributed to evaporable water in the ash, but it is not prominent because the ash was dried before analysis. The second peak, at about 400–500 °C, is caused by the dehydration of portlandite [37]. The portlandite peak is the most visible in ashes 4, 6, and 8 after CO<sub>2</sub> exposure at lower RHs (Figure 6b), while this peak is no longer visible after CO<sub>2</sub> exposure at higher RHs (Figure 7b), as is consistent with previous XRD analyses. The third peak, which contributes to the mass loss in the temperature range from 550 °C to 950 °C, results from the decomposition of CaCO<sub>3</sub> into CaO and the release of CO<sub>2</sub> (Equation (7)). The weight loss in this range is higher for carbonated samples, thus confirming that the carbonation process was successful [34].



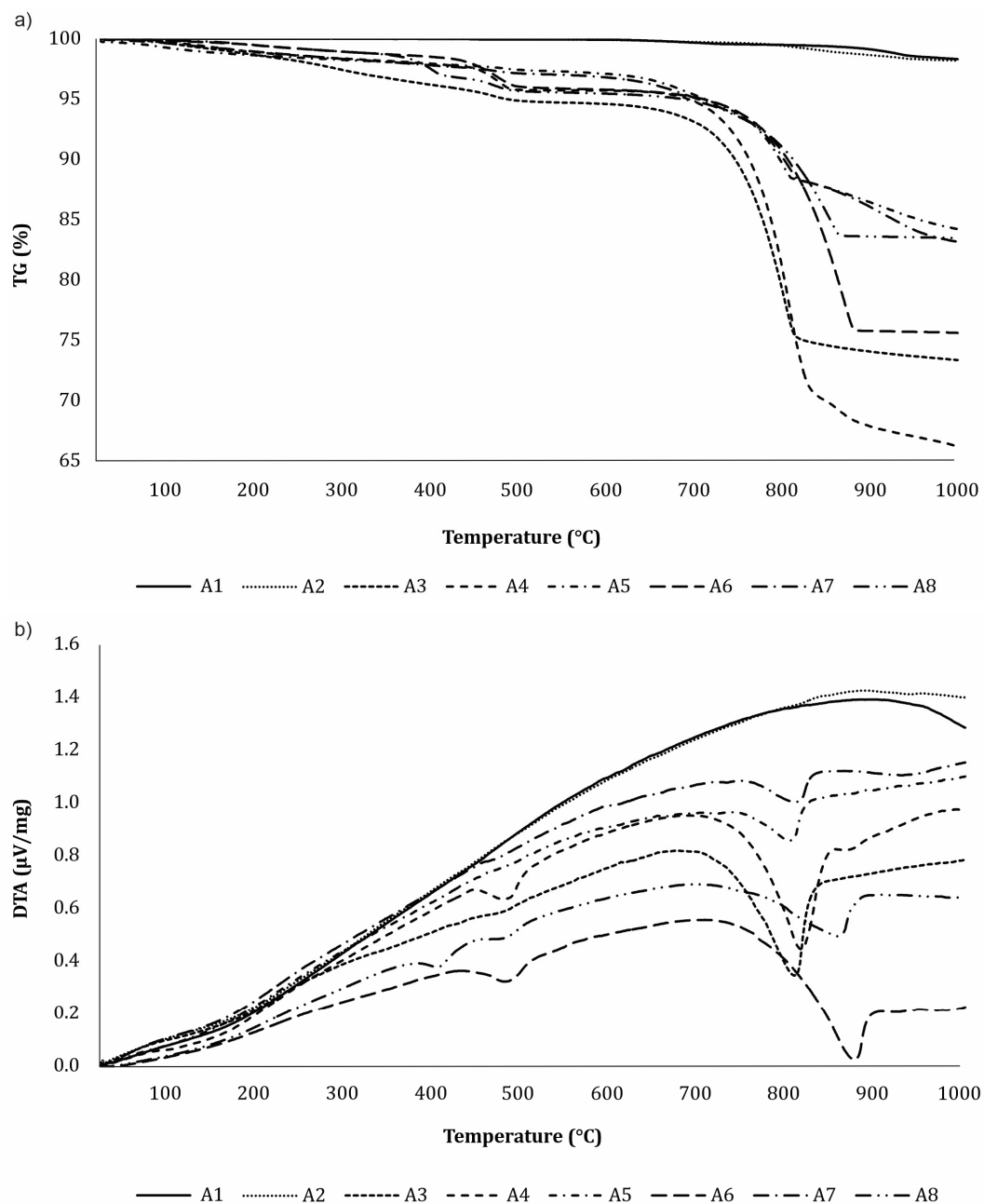


**Figure 6.** (a) TG analysis and (b) DTA analysis for carbonated ashes after 28 days of CO<sub>2</sub> exposure at an RH of 50–55%.

A DTA analysis can distinguish the decomposition of portlandite and calcite, a task which is not possible using the mass gain method. The CaCO<sub>3</sub> decomposition peak was observed in all ashes except the coal fly ashes (A1 and A2), indicating that these ashes have no potential for CO<sub>2</sub> sequestration, as expected. After 28 days of CO<sub>2</sub> exposure at an RH of 80–85%, the biomass ashes A3 (21.3%) and A4 (33.8%) and mixed ash from the paper mill A6 (28.8%) had the greatest CO<sub>2</sub> sequestration potential of the analyzed ashes. Both the fly ashes from the paper mill (A5) and from the co-combustion of brown coal and biomass wood chips sequester 15.9% of CO<sub>2</sub>, while bottom ash from the Slovenian heating and power station (A8) sequesters 13.7%. At a lower RH, the CO<sub>2</sub> sequestration capacity is slightly lower for all ashes due to incomplete carbonation (Table 2).

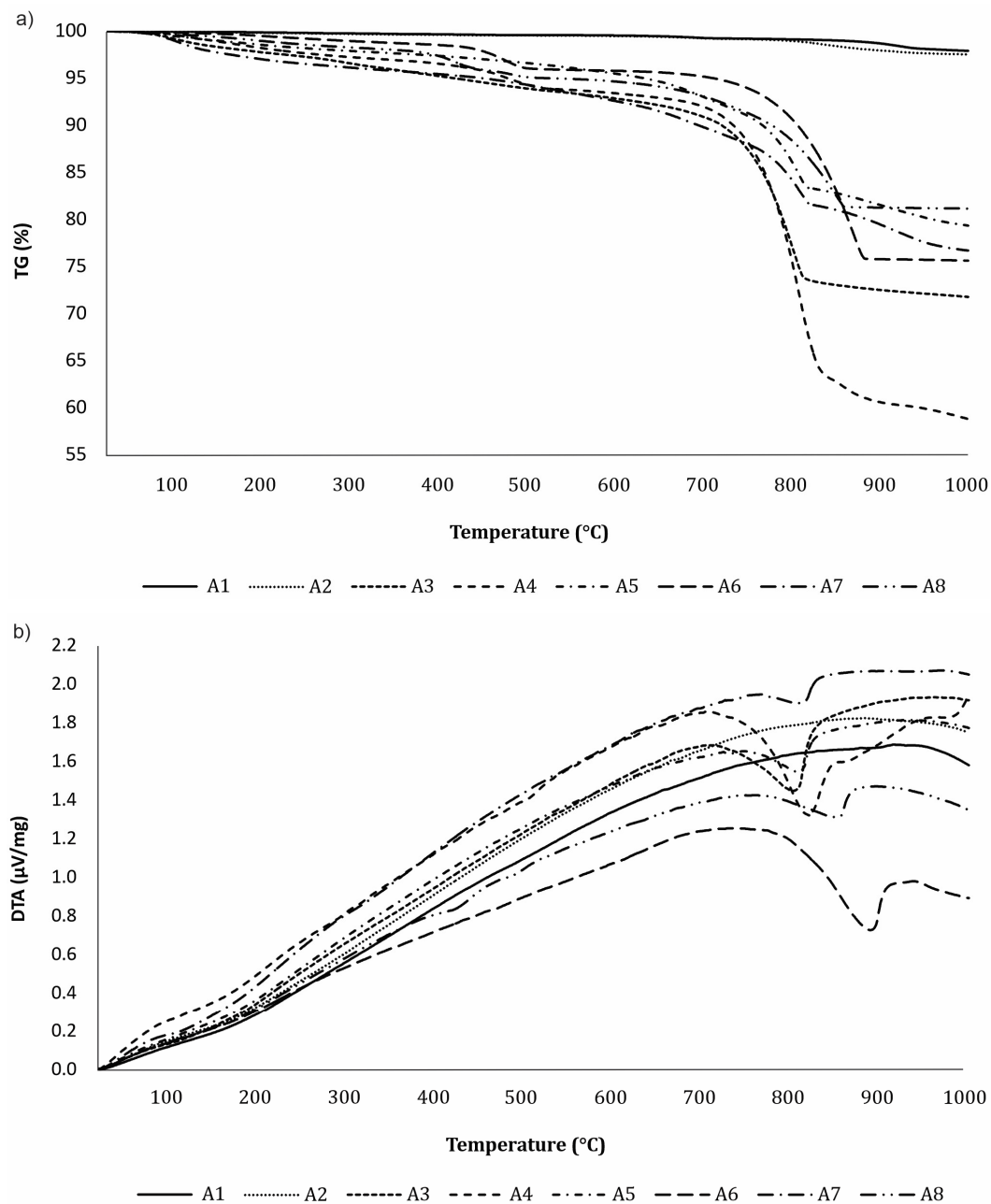


**Figure 7.** (a) TG analysis and (b) DTA analysis for carbonated ashes after 28 days of CO<sub>2</sub> exposure at an RH of 80–85%.

**Table 2.** Mass uptake ( $mass_{\text{uptake}}$ ), CO<sub>2</sub> sequestration capacity determined by TG analysis ( $CO_{2\text{-TG exp}}$ ), theoretical maximum of sequestered CO<sub>2</sub> according to the Steinhour equation ( $CO_{2\text{-max}}$ ), and calculated carbonation efficiency (CE) after 28 days of exposure at RH of 50–55%.

Ash	$mass_{\text{uptake}}$ (%)	$CO_{2\text{-TG exp}}$ (%)	$CO_{2\text{-max}}$ (%)	CE (%)
A1	0.1	1.4	9.8	14.2
A2	0.2	1.6	13.3	12.3
A3	1.7	21.0	32.6	64.4
A4	9.0	28.7	49.8	57.6
A5	5.9	12.2	34.3	35.4
A6	9.9	20.2	46.5	43.3
A7	4.2	12.9	26.0	49.5
A8	5.5	12.0	37.7	31.8

In general, the total CO<sub>2</sub> release depends on the ash type. Ashes with a higher CaO content in their chemical composition (see Table 1) have a greater CO<sub>2</sub> sequestration potential, which is also reflected in a higher mass loss in the TG diagram.

### 3.4. CO<sub>2</sub> Sequestration Capacity and Carbonation Efficiency (CE)

The CO<sub>2</sub> sequestration capacity and calculated carbon efficiency for all ashes after 28 days of accelerated carbonation in a 4% CO<sub>2</sub> environment at RH of 50–55% are presented in Table 2 and at an RH of 80–85% in Table 3. The highest percentage of sequestered CO<sub>2</sub> (33.8%) and mass uptake (17.3%) was found in bottom ash from wood biomass (A4), which corresponds to a CE of 67.9%, as presented in Table 3 and Figure 8. This means that the ash A4 can sequester 67.9% of the maximum theoretical mass by using the Steinoor stoichiometric formula [13,16,23,37]. For fly ash from wood biomass (A3), 65.2% CE was achieved, with 21.3% sequestered CO<sub>2</sub>, while the theoretical maximum of sequestered CO<sub>2</sub> was 32.6%. However, a minimum mass uptake was measured here, indicating that the ash was already carbonized, probably due to a long-term natural carbonation before sampling [15]. The storage and transport conditions of WBA largely determine the amount of CaO and other carbonates, as carbonation and hydration can occur during these processes under moist conditions. Upon contact with water/moisture, up to 50% of the CaO content of WBA reacts to form Ca(OH)<sub>2</sub>, which, in turn, reacts to CaCO<sub>3</sub> upon contact with CO<sub>2</sub> [40].

**Table 3.** Mass uptake (mass<sub>uptake</sub>), CO<sub>2</sub> sequestration capacity determined by TG analysis (CO<sub>2-TG exp</sub>), theoretical maximum of sequestered CO<sub>2</sub> according to the Steinoor equation (CO<sub>2-max</sub>), and calculated carbonation efficiency (CE) after 28 days of exposure at RH of 80–85%.

Ash	mass <sub>uptake</sub> (%)	CO <sub>2-TG exp</sub> (%)	CO <sub>2-max</sub> (%)	CE (%)
A1	0.2	1.5	9.8	15.0
A2	0.5	1.9	13.3	14.2
A3	5.0	21.3	32.6	65.2
A4	17.3	33.8	49.8	67.9
A5	11.8	15.9	34.3	46.3
A6	20.4	28.8	46.5	61.9
A7	11.1	15.9	26.0	61.2
A8	7.6	13.7	37.7	36.4

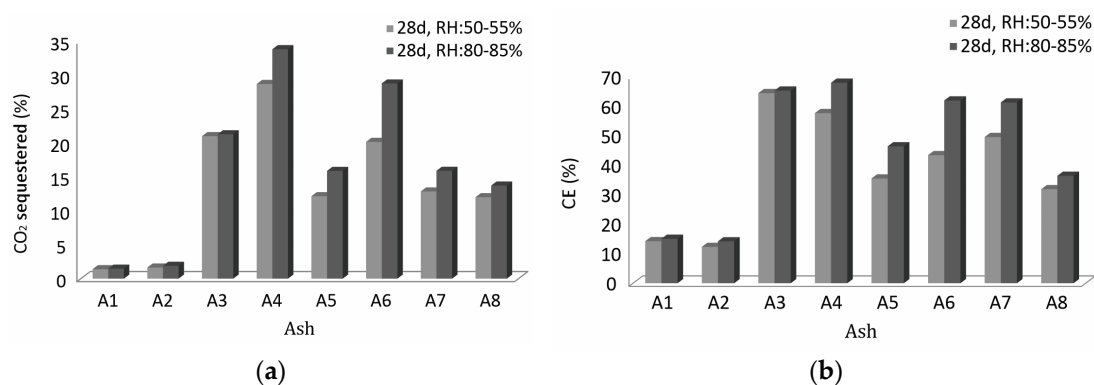


**Figure 8.** (a) Percentage of sequestered CO<sub>2</sub> determined by TG after 28 days of CO<sub>2</sub> exposure at RH of 50–55% and 80–85% and (b) calculated carbonation efficiency at RH of 50–55% and 80–85% for all ashes.

The mixed ash from the paper mill (A6) sequesters 28.8% of CO<sub>2</sub>, resulting in the highest mass uptake (20.4%) and a CE of 61.9% (Table 3). The CE for fly ash from the same paper mill (A5) was 46.3%. Although A6 is 90% bottom ash and has a broad particle size distribution [45], it is very reactive to CO<sub>2</sub>, contradicting the claim that the fine fly-ash particles are more reactive to CO<sub>2</sub> than bottom ash [23]. The particle size of an ash should

not always be considered a limiting factor for CO<sub>2</sub> sequestration, but, in general, ashes with a similar chemical composition have a higher carbonation efficiency at smaller particle sizes [15,23,46]. However, if the calcium content of the feedstock varies, the particle size or surface area may be of secondary importance [32].

The presented approach is suitable for waste ashes with a high Ca content. Both types of coal fly ash (A1 and A2) showed neither sequestration potential nor high carbonation efficiency. Nevertheless, the average CE after 28 days of CO<sub>2</sub> exposure at an RH of 80–85% was 66.6% for WBA, which is much higher than in the study reported by Koch et al. [13]. Most WBA is still landfilled, and disposal costs are high, so a direct use of the ash for CO<sub>2</sub> sequestration would be beneficial in terms of a circular economy [13].

In further studies, it would be optimal to shorten the processing time by optimizing the carbonation conditions; however, these results open the possibility for future studies using the proposed methodology. To quantify the environmental impact, a life-cycle analysis could also be the subject of future studies.

#### 4. Conclusions

This study focused on determining the sequestration potential of the waste ashes in a CO<sub>2</sub> direct mineral carbonation process using a number of complementary analytical methods. To understand the reaction kinetics, we determined the appropriate conditions for accelerated carbonation. Using XRD and DTA, we followed the carbonation of portlandite and lime at different RHs (50–55% and 80–85%) and monitored the CaCO<sub>3</sub> content with calcimetric measurements. The sequestration capacity was determined by TG, and the carbonation efficiency was calculated for each ash.

The obtained results showed that the reaction rate increased with increasing RH, and the maximum carbonation was achieved after 28 days in a dense carbonation chamber with 4% *v/v* CO<sub>2</sub>, a temperature of 20 °C, and an RH of 80–85%. Ca-rich waste ashes were successfully used for direct mineral carbonation, with the highest carbonation efficiency (67.9%) and sequestration capacity (33.8%) achieved with wood biomass bottom ash (A4). In addition, we showed that wood ash is highly reactive to CO<sub>2</sub>, so its direct use for CO<sub>2</sub> sequestration would be beneficial in terms of a circular economy because 70% of wood biomass ash is still landfilled.

**Author Contributions:** Conceptualization, V.D.; methodology, S.T. and V.D.; validation, S.T. and V.D.; investigation, S.T.; writing—original draft preparation, S.T.; writing—review and editing, V.D.; supervision, V.D. All authors have read and agreed to the published version of the manuscript.

**Funding:** This research was EU-funded by ASHCYCLE project, grant number 101058162.

**Institutional Review Board Statement:** Not applicable.

**Informed Consent Statement:** Not applicable.

**Data Availability Statement:** The data presented in this study are openly available from the repository DiRRROS: <http://hdl.handle.net/20.500.12556/DiRRROS-16698> (accessed on 20 July 2023), and upon request from the first and corresponding author.

**Conflicts of Interest:** The authors declare no conflict of interest.

#### References

1. Pacheco-Torgal, F. Introduction to carbon dioxide sequestration-based cementitious construction materials. In *Carbon Dioxide Sequestration in Cementitious Construction Materials*; Elsevier Ltd.: Amsterdam, The Netherlands, 2018; pp. 3–12. [CrossRef]
2. Alturki, A. The Global Carbon Footprint and How New Carbon Mineralization Technologies Can Be Used to Reduce CO<sub>2</sub> Emissions. *ChemEngineering* **2022**, *6*, 44. [CrossRef]
3. Leung, D.Y.C.; Caramanna, G.; Maroto-Valer, M.M. An overview of current status of carbon dioxide capture and storage technologies. *Renew. Sustain. Energy Rev.* **2014**, *39*, 426–443. [CrossRef]
4. Betts, R.A.; Jones, C.D.; Knight, J.R.; Keeling, R.F.; Kennedy, J.J. El Niño and a record CO<sub>2</sub> rise. *Nat. Clim. Chang.* **2016**, *6*, 806–810. [CrossRef]

5. Stern, N. *The Economics of Climate Change: The Stern Review*; Cambridge University Press: Cambridge, UK, 2006; pp. 1–692. [[CrossRef](#)]
6. Liu, Z.; Ciais, P.; Deng, Z.; Lei, R.; Davis, S.J.; Feng, S.; Zheng, B.; Cui, D.; Dou, X.; Zhu, B.; et al. Near-real-time monitoring of global CO<sub>2</sub> emissions reveals the effects of the COVID-19 pandemic. *Nat. Commun.* **2020**, *11*, 1–12. [[CrossRef](#)]
7. Le Quéré, C.; Jackson, R.B.; Jones, M.W.; Smith, A.J.; Abernethy, S.; Andrew, R.M.; De-Gol, A.J.; Willis, D.R.; Shan, Y.; Canadell, J.G.; et al. Temporary reduction in daily global CO<sub>2</sub> emissions during the COVID-19 forced confinement. *Nat. Clim. Chang.* **2020**, *10*, 647–653. [[CrossRef](#)]
8. Liu, Z.; Deng, Z.; Davis, S.J.; Giron, C.; Ciais, P. Monitoring global carbon emissions in 2021. *Nat. Rev. Earth Environ.* **2022**, *3*, 217–219. [[CrossRef](#)]
9. Garcia, J.A.; Villen-Guzman, M.; Rodriguez-Maroto, J.M.; Paz-Garcia, J.M. Technical Analysis of CO<sub>2</sub> Capture Pathways and Technologies. *J. Environ. Chem. Eng.* **2022**, *10*, 108470. [[CrossRef](#)]
10. Carbon Dioxide | Vital Signs—Climate Change: Vital Signs of the Planet. Available online: <https://climate.nasa.gov/vital-signs/carbon-dioxide/> (accessed on 3 April 2023).
11. Xie, W.; Li, H.; Yang, M.; He, L.; Li, H. CO<sub>2</sub> capture and utilization with solid waste. *Green Chem. Eng.* **2022**, *3*, 199–209. [[CrossRef](#)]
12. Meylan, F.D.; Moreau, V.; Erkman, S. CO<sub>2</sub> utilization in the perspective of industrial ecology, an overview. *J. CO<sub>2</sub> Util.* **2015**, *12*, 101–108. [[CrossRef](#)]
13. Koch, R.; Sailer, G.; Paczkowski, S.; Pelz, S.; Poetsch, J.; Müller, J. Lab-Scale Carbonation of Wood Ash for CO<sub>2</sub>—Sequestration. *Energies* **2021**, *14*, 7371. [[CrossRef](#)]
14. Vassilev, S.V.; Vassileva, C.G.; Petrova, N.L. Mineral Carbonation of Biomass Ashes in Relation to Their CO<sub>2</sub> Capture and Storage Potential. *ACS Omega* **2021**, *6*, 14598–14611. [[CrossRef](#)] [[PubMed](#)]
15. Li, L.; Wu, M. An overview of utilizing CO<sub>2</sub> for accelerated carbonation treatment in the concrete industry. *J. CO<sub>2</sub> Util.* **2022**, *60*, 102000. [[CrossRef](#)]
16. Ashraf, W. Carbonation of cement-based materials: Challenges and opportunities. *Constr. Build. Mater.* **2016**, *120*, 558–570. [[CrossRef](#)]
17. Ekolu, S.O. A review on effects of curing, sheltering, and CO<sub>2</sub> concentration upon natural carbonation of concrete. *Constr. Build. Mater.* **2016**, *127*, 306–320. [[CrossRef](#)]
18. Lippiatt, N.; Ling, T.C.; Pan, S.Y. Towards carbon-neutral construction materials: Carbonation of cement-based materials and the future perspective. *J. Build. Eng.* **2020**, *28*, 101062. [[CrossRef](#)]
19. Saran, R.K.; Arora, V.; Yadav, S. CO<sub>2</sub> sequestration by mineral carbonation: A review. *Glob. Nest J.* **2018**, *20*, 497–503. [[CrossRef](#)]
20. Liu, W.; Su, S.; Xu, K.; Chen, Q.; Xu, J.; Sun, Z.; Wang, Y.; Hu, S.; Wang, X.; Xue, Y.; et al. CO<sub>2</sub> sequestration by direct gas–solid carbonation of fly ash with steam addition. *J. Clean. Prod.* **2018**, *178*, 98–107. [[CrossRef](#)]
21. Olajire, A.A. A review of mineral carbonation technology in sequestration of CO<sub>2</sub>. *J. Pet. Sci. Eng.* **2013**, *109*, 364–392. [[CrossRef](#)]
22. Costa, G.; Baciocchi, R.; Polettoni, A.; Pomi, R.; Hills, C.D.; Carey, P.J. Current status and perspectives of accelerated carbonation processes on municipal waste combustion residues. *Environ. Monit. Assess.* **2007**, *135*, 55–75. [[CrossRef](#)]
23. Nam, S.Y.; Seo, J.; Thriveni, T.; Ahn, J.W. Accelerated carbonation of municipal solid waste incineration bottom ash for CO<sub>2</sub> sequestration. *Geosyst. Eng.* **2012**, *15*, 305–311. [[CrossRef](#)]
24. Hjelm, O.; Hyks, J.; Korpijärvi, K.; Wahlström, R.; Grönholm, M. BAT (Best Available Techniques) for Combustion and Incineration Residues in a Circular Economy. Available online: <https://pub.norden.org/temanord2022-542/#> (accessed on 30 September 2022).
25. Shih, S.M.; Ho, C.S.; Song, Y.S.; Lin, J.P. Kinetics of the reaction of Ca(OH)<sub>2</sub> with CO<sub>2</sub> at low temperature. *Ind. Eng. Chem. Res.* **1999**, *38*, 1316–1322. [[CrossRef](#)]
26. Steiner, S.; Lothenbach, B.; Proske, T.; Borgschulte, A.; Winnefeld, F. Effect of relative humidity on the carbonation rate of portlandite, calcium silicate hydrates and ettringite. *Cem. Concr. Res.* **2020**, *135*, 106116. [[CrossRef](#)]
27. Ebrahimi, A.; Safari, M.; Milani, D.; Montoya, A.; Valix, M.; Abbas, A. Sustainable transformation of fly ash industrial waste into a construction cement blend via CO<sub>2</sub> carbonation. *J. Clean. Prod.* **2017**, *156*, 660–669. [[CrossRef](#)]
28. Shao, Y.; El-Hassan, H. CO<sub>2</sub> Utilization in Concrete. In Proceedings of the Third International Conference on Sustainable Construction Materials and Technologies (SCMT3), Kyoto, Japan, 18–22 August 2013; Available online: [https://www.researchgate.net/publication/285871693\\_CO2\\_Utilization\\_in\\_Concrete](https://www.researchgate.net/publication/285871693_CO2_Utilization_in_Concrete) (accessed on 25 March 2023).
29. First Footpath Constructed with Carbstone Clinkers—VITO. Available online: <https://vito.be/en/news/first-footpath-constructed-carbstone-clinkers> (accessed on 8 May 2023).
30. Kamyab, H.K.; Nielsen, P.; Van Mierloo, P.; Horckmans, L. Carbstone pavers: A sustainable solution for the urban environment. *Appl. Sci.* **2021**, *11*, 6418. [[CrossRef](#)]
31. Winnefeld, F.; Leemann, A.; German, A.; Lothenbach, B. CO<sub>2</sub> storage in cement and concrete by mineral carbonation. *Curr. Opin. Green Sustain. Chem.* **2022**, *38*, 100672. [[CrossRef](#)]
32. Tripathi, N.; Hills, C.D.; Singh, R.S.; Singh, J.S. Offsetting anthropogenic carbon emissions from biomass waste and mineralised carbon dioxide. *Sci. Rep.* **2020**, *10*, 958. [[CrossRef](#)]
33. Ukrainczyk, N.; Vrbos, N.; Koenders, E.A.B. Reuse of woody biomass ash waste in cementitious materials. *Chem. Biochem. Eng. Q.* **2016**, *30*, 137–148. [[CrossRef](#)]

34. Tamilselvi Dananjayan, R.R.; Kandasamy, P.; Andimuthu, R. Direct mineral carbonation of coal fly ash for CO<sub>2</sub> sequestration. *J. Clean. Prod.* **2016**, *112*, 4173–4182. [[CrossRef](#)]
35. EN 196-2:2013; Method of Testing Cement—Part 2: Chemical Analysis of Cement. CEN: Brussels, Belgium, 2013.
36. EN 451-1:2017; Method of Testing Fly Ash—Part 1: Determination of Free Calcium Oxide Content. CEN: Brussels, Belgium, 2017.
37. Nedeljković, M.; Ghiassi, B.; Melzer, S.; Kooij, C.; van der Laan, S.; Ye, G. CO<sub>2</sub> binding capacity of alkali-activated fly ash and slag pastes. *Ceram. Int.* **2018**, *44*, 19646–19660. [[CrossRef](#)]
38. Domingo, M.; Vicente, F.-A.; Aparicio, P. Proposed Methodology to Evaluate CO<sub>2</sub> Capture Using Construction and Demolition Waste. *Minerals* **2019**, *6*, 612. [[CrossRef](#)]
39. Neeraj; Yadav, S. Carbon storage by mineral carbonation and industrial applications of CO<sub>2</sub>. *Mater. Sci. Energy Technol.* **2020**, *3*, 494–500. [[CrossRef](#)]
40. Ayobami, A.B. Performance of wood bottom ash in cement-based applications and comparison with other selected ashes: Overview. *Resour. Conserv. Recycl.* **2021**, *166*, 105351. [[CrossRef](#)]
41. Possan, E.; Thomaz, W.A.; Aleandri, G.A.; Felix, E.F.; dos Santos, A.C.P. CO<sub>2</sub> uptake potential due to concrete carbonation: A case study. *Case Stud. Constr. Mater.* **2017**, *6*, 147–161. [[CrossRef](#)]
42. Dheilily, R.M.; Tudo, J.; Sebaibi, Y.; Quéneudec, M. Influence of storage conditions on the carbonation of powdered Ca(OH)<sub>2</sub>. *Constr. Build. Mater.* **2002**, *16*, 155–161. [[CrossRef](#)]
43. Galan, I.; Glasser, F.P.; Baza, D.; Andrade, C. Assessment of the protective effect of carbonation on portlandite crystals. *Cem. Concr. Res.* **2015**, *74*, 68–77. [[CrossRef](#)]
44. Fernández, R.G.; García, C.P.; Lavín, A.G.; Bueno De Las Heras, J.L. Study of main combustion characteristics for biomass fuels used in boilers. *Fuel Process. Technol.* **2012**, *103*, 16–26. [[CrossRef](#)]
45. Kramar, S.; Ducman, V. Evaluation of ash pozzolanic activity by means of the strength activity index test, Frattini test and DTA/TG analysis. *Teh. Vjesn.* **2018**, *25*, 1746–1752. [[CrossRef](#)]
46. Ukwattage, N.L.; Ranjith, P.G.; Yellishetty, M.; Bui, H.H.; Xu, T. A laboratory-scale study of the aqueous mineral carbonation of coal fly ash for CO<sub>2</sub> sequestration. *J. Clean. Prod.* **2015**, *103*, 665–674. [[CrossRef](#)]

**Disclaimer/Publisher's Note:** The statements, opinions and data contained in all publications are solely those of the individual author(s) and contributor(s) and not of MDPI and/or the editor(s). MDPI and/or the editor(s) disclaim responsibility for any injury to people or property resulting from any ideas, methods, instructions or products referred to in the content.